New Device for Continuous-Wave THz Emission: Large Area Emitter

Luis Enrique García-Muñoz , Gottfried Döhler , Javier Montero-de-Paz , Eduardo Ugarte-Muñoz , Alejandro Rivera-Lavado , Sascha Preu , Stefan Malzer , Sebastian Bauerschmidt , Vicente Gonzalez-Posadas , Daniel Segovia-Vargas

***Abstract*— We discuss two different approaches to overcome the power limitations of CW THz generation imposed to conventional photomixers. The increase in power achievable by using arrays of AEs is studied. Then "large area emitters" are proposed as an alternate approach to overcome the power limitations. In this antenna-free new scheme of photomixing, the THz radiation originates directly from the acceleration of photo-induced charge carriers generated within a large semiconductor area. The quasi-continuous distribution of emitting elements corresponds to a high-density array and results in particularly favorable radiation profiles.**

I. INTRODUCTION

The well-established method of generation of continuous-wave Terahertz (CW-THz) radiation by photomixing [1] consists of two basic steps. Two laser beams, slightly differing in their frequencies (the desired THz frequency), are generating a THz photocurrent in a semiconductor device. This current is fed into an antenna, deposited onto the (semi-insulating, THz-transparent) semiconductor substrate, which then emits THz radiation with high efficiency, provided the antenna design is suitable for the chosen THz frequency. The major fraction of the THz power is radiated into the substrate, due to the much smaller wave impedance of semiconductors, attributed to their high dielectric constant. For convenient collection and collimation of the radiation, a hyper-hemispherical lens, fabricated from a material with similar dielectric constant, is placed below the substrate at the symmetry centre of the antenna (Figure 1).

II. ANTENNA EMITTER (AE) APPROACH

In Figure 2 the numerically calculated angular radiation intensity emitted by an AE with horizontal $\lambda/2$ dipole antenna of length 42µm at 1 THz placed along the x-axis into the substrate, obtained from the analytical formulation based on Helmholtz's potentials, is shown for the E-plane and the H-plane. Results are consistent with the ones presented [2]-[4]. It has to be pointed out that the backward radiation (radiation into the air) is not plotted in order to have a friendlier picture.

The radiation intensity can be strongly enhanced by the use of a suitably designed hyperhemispherical lens fabricated from a material with a refractive index similar to that of the semiconductor, $n_{sc} \approx 3.5$. At the same time the lens allows collecting nearly all the radiation emitted into the semiconductor. Without the lens, the radiation emitted under an angle exceeding the critical angle for total reflection $\theta_c = \arcsin(1/n_{sc}) \approx 16^\circ$ could not be extracted. The blue full line in Figure 2 depicts the simulated angular radiation intensity for the AE with lens, again for the E-plane and for the H-plane for the same AE as before, but with a lens of radius $R_l = 2$ mm. The lens has been analyzed with Physical Optics (PO) following the same methodology proposed by Filipovic in [5], taking into account the total internal reflection at the second semiconductor-air interface, where the THz beam leaves the substrate. The radiation intensity at $\theta = 0^\circ$ is increased by 24.38dB while the 3 dB angle is reduced from 47.72° to 2.4°. We note that the intensity pattern does not significantly differ from the diffraction-limited pattern of an Airy disk of the same diameter [6].

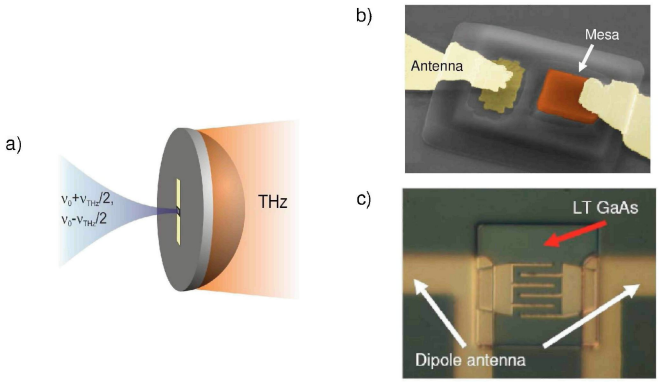

Figure 1. (a) Schematic picture of an antenna emitter. The two laser beams (blue online) are focused onto the small semiconductor device between the arms of the antenna (yellow online). The THz radiation (reddish online) emitted into the semiconductor substrate (online blue-gray), transmitted into the (hemi)spherical lens and, finally, into the air. (b) p-i-n diode based device with top and bottom contacts connected to the antenna arms (c) Photoconductive mixer device with interdigitated contacts deposited on low-temperature grown GaAs (LT-GaAs).

The total THz power, P_{THz}, which can be generated with a single AE (at a given frequency), is limited by the design of the photoconductive or pin photomixer semiconductor device.

These restrictions limit the THz power achievable with a single AE (nowadays) to about $P_{THz} < 10$ µW for AEs with resonant and to a few µW in the case of broad-band antennas at 1 THz. The most straight-forward solution to achieve an increase in THz power from photomixers is using an array.

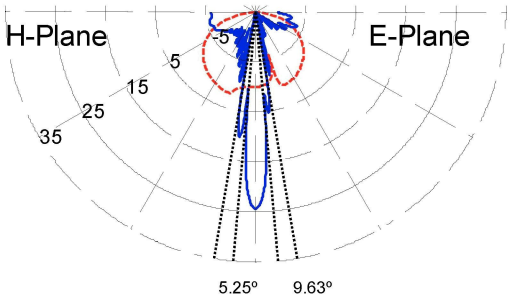

Figure 2. Calculated angular radiation intensity emitted by an AE with λ/2 dipole antenna of length 42µm at 1THz, without and with lens. Dipole without lens (dashed line, red) lying in the interface of a semi-infinite semiconductor and dipole with 2mm radius and 0.69mm slab hyperhemispherical lens (full line, blue).

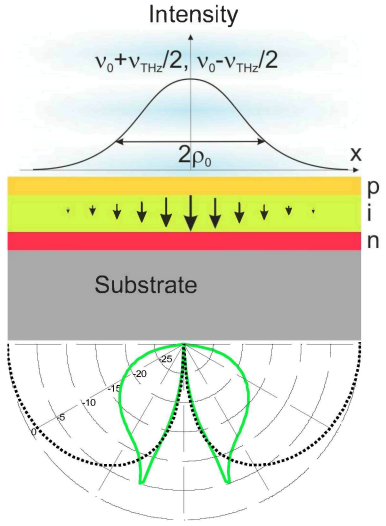

(a)

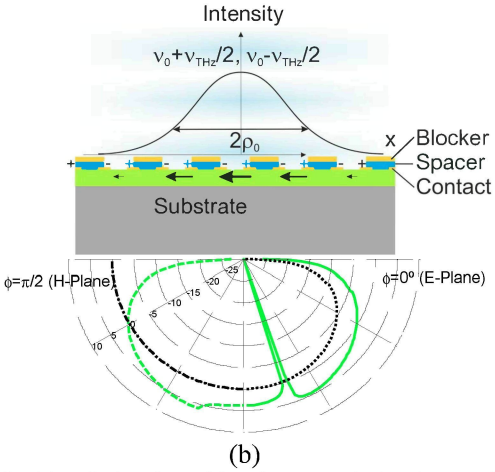

(b)

Figure 3. (a)Radiation intensities for a vertical LAE at the interface, (b)Radiation intensities for a horizontal LAE at the interface.

III. LARGE AREA EMITTER

In this antenna-free new scheme of photomixing the THz radiation originates directly from the acceleration of photo-induced charge carriers generated within a large semiconductor area. The quasi-continuous distribution of emitting elements corresponds to a high-density array and results in favorable radiation profiles without side lobes. Moreover, the achievable THz power is expected to outnumber even large AEAs. Last not least, the technological challenge of fabricating LAEs appears to be significantly less demanding.

In Figure 3 the radiation intensities for (a) the vertical and (b) the horizontal LAE at the interface are shown (full and dash- lines) and compared with those of the corresponding LAE embedded in the semiconductor (dashed-dotted and dotted lines), renormalized to the maximum power emitted by the dipole embedded into the semiconductor perpendicular to its axis. The effect of the interface is most pronounced for the vertical dipole (Figure 3(a)). As expected, most of the power is emitted into the semiconductor. Its total emitted power is strongly reduced compared with the embedded dipole. The radiation intensity radiated into the semiconductor exhibits a pronounced maximum at the critical angle for total reflection $\theta = \theta c$. Even at this maximum the radiation intensity is only the fraction $4/n_{sc}^2 \approx 31\%$ of the maximum value, which would be expected for $\theta = 90°$ for the dipole embedded in the semiconductor. In the range $\theta_c < \theta < \pi/2$ the radiation intensity of the dipole at the interface decreases monotonically and becomes zero at $\theta = \pi/2$, where it would reach its maximum for the embedded dipole. The changes of the power distribution are less pronounced for the horizontal LAE (Figure 3(b)). Here, the maximum is found in the H-plane ($\varphi=\pi/2$) at $\theta = \theta_c$. Its value corresponds to 4 times the power expected at $\theta = 0$ for the horizontal embedded LAE. In the E-plane ($\varphi=\pi/2$), in contrast, zero power is expected at $\theta = \theta_c$.

higher total laser power can be applied without the risk of thermal failure and without causing screening if an alternative THz emitter concept is found that allows for the laser power to be spread over a large area comparable with the size of the antenna, or even larger. Such a “large area emitter” (LAE) concept (Fig.1(a) and Fig.1(b)) can be implemented by taking advantage of the fact that the charge carriers generated in the semiconductor become elementary Hertzian dipole sources of THz radiation, if subjected to an accelerating DC electric field $\mathbf{E_0}$. The THz fields of the dipole interfere constructively and the radiated power increases with laser power quadratically, as in the case of antenna emitters, if the area, in which the carriers are generated, is small compared with the THz wavelength [2]. The angular distribution of the THz power will be the same as that for an elementary dipole in this case (“large area quasi dipole” (LAQD)). If, however, the size of the illuminated area becomes comparable with the THz wavelength or even larger, interference effects will become essential and the radiation pattern will become more narrow. Like in an array of THz antennas, we will find that the maximum radiation intensity still increases quadratically with laser power for the direction of coherent superposition, whereas the total THz power only increases proportional to the

laser power, due to correspondingly decreasing beam width in the extreme large area limit, if the array dimensions significantly exceed the THz wavelength.

A single electron in a semiconductor of dielectric constant ε_{sc}, characterized by an effective mass m_c (typically $m_c \approx (0.04 \ldots 0.07)m_0$, where $m_0 = 9.1\text{x}10^{-31}$ kg is the mass of a free electron), emits a THz pulse if accelerated by an electric field $\mathbf{E_0}$. The total THz power $P_{THz}(t)$ is given by [1-4]

$$P_{e\_THz}(t) = \left(\frac{Z_0}{6\cdot\pi}\right)\cdot\frac{e^2\cdot[a(t)]^2\cdot n_{sc}}{c^2} \qquad (1)$$

Here, e = 1.602 x 10^{-19} C as is the elementary charge, c = 3 x 10^{10} cm/s the vacuum velocity of light, $Z_0 = (\varepsilon_0 c)^{-1} = 376.73$ Ω the impedance of free space and $n_{sc} = (\varepsilon_{sc})^{1/2}$ the refractive index of the semiconductor). In typical III-V semiconductors and at sufficiently high electric fields (> 3 kV/cm) the time dependent acceleration *a(t)* can be approximated by an initial "ballistic" acceleration $\mathbf{a_1} = e\mathbf{E}_0/m_c$ up to a maximum ballistic velocity of about $v_{bal}^{max} \approx 10^8$cm/s (in GaAs) and $2\text{x}10^8$cm/s (in InGaAs, e.g.), followed by a deceleration due to scattering, which can be approximated by $\mathbf{a_2} = -\mathbf{a_1}$ [2],[9]. The superposition of the transient THz fields of the carriers generated by the modulated laser power $P_L(t)$ yields in the LAQD-limit

$$P_{THz}^{LAQD} = \frac{1}{2}\cdot R_{LAQD}\cdot\left|I_{THz}(\omega_{THz})\right|^2 \qquad (2)$$

with

$$R_{LAQD} = \left(\frac{2\cdot Z_0\cdot n_{sc}}{3\cdot\pi}\right)\cdot\left(\frac{v_{bal}}{c}\right)^2 = (3.2\ldots12.8)\cdot10^{-3}\,\Omega$$

$$\text{for } v_{bal} = (1\ldots2)\cdot10^8\, cm/s \qquad (3)$$

and

$$I_{THz}(\omega_{THz}) = I_{0,pin}\cdot f(\omega_{THz}) \qquad (4)$$

The frequency dependent factor

$$f(\omega_{THz}) = \frac{(1-\cos(\omega_{THz}\cdot\tau_{bal}))}{\omega_{THz}\cdot\tau_{bal}} \qquad (5)$$

linearly increases with $\omega_{THz}\tau_{bal}$ at low frequencies, reaches the maxima at about $\omega_{THz}\tau_{bal} \approx (¾)\pi$ and $(2n+1)\pi$ and the minima at $\omega_{THz}\tau_{bal} \approx 2n\pi$ (n = 1, 2, 3, …) . This behavior reflects the fact that, at low THz frequencies ($\omega_{THz} << \tau_{bal}^{-1}$), the fields of accelerated carriers are strongly reduced due to destructive interference with the opposite fields of decelerated, previously generated carriers, as the acceleration and deceleration times, $\tau_{bal} \approx v_{bal}/a_1 = v_{bal}m_c/eE_0$, are short compared to the THz period, $T_{THz} = 1/\nu_{THz}$. The main maximum of $f(\omega_{THz} = 3\pi/4\tau_{bal}) \approx 0.72$ occurs close to the frequency at which the acceleration and deceleration times, v_{bal}, closely correspond to half a THz period T_{THz}. The ballistic acceleration time $\tau_{bal} = v_{bal}/a = v_{bal}m_c/eE_0$ can be adapted to fulfill the condition for maximum THz power, $\tau_{bal} = (3/8)\,T_{THz} = (3/8\nu_{THz})$. This condition yields 6 kV/cm < E_0 < 60 kV/cm for 0.5 THz < ν_{THz} < 5 THz for InGaAs, e.g. For the optimum adapted fields the THz power becomes

$$P_{THz}^{LAQD} = \frac{1}{2}\cdot(1.76\ldots6.7)\cdot10^{-3}\,\Omega\cdot I_{pin}^2, \qquad \text{for } v_{bal} = (1\ldots2)\cdot10^8\, cm/s \qquad (6)$$

The angular dependence of the radiation intensity, i.e. the power emitted per space angle element $d\Omega=\sin\theta\, d\theta\, d\varphi$, is the same for a LAQD as for a Hertzian dipole in the far-field. It increases quadratically with the sine of the angle between the accelerating DC-field $\mathbf{E_0}$ and the vector $\mathbf{r}$ from the center of the LAE device to the observation point. For a field in z-direction, $\mathbf{E_0} = E_0\,(0, 0, 1)$, this angle is identical with the polar angle θ and one obtains for the radiation intensity

$$U_v^{LAQD}(\theta) = \left(\frac{3}{8\cdot\pi}\right)\cdot P_{THz}^{LAQD}\cdot\sin^2(\theta) \qquad (7)$$

whereas, for a field in x-direction, $\mathbf{E_0} = E_0\,(1, 0, 0)$ the radiation intensity depends on both the polar angle θ and the azimuth angle φ

$$U_h^{LAQD}(\theta,\varphi) = \left(\frac{3}{8\cdot\pi}\right)\cdot P_{THz}^{LAQD}\cdot\left(1-\sin^2(\theta)\cdot\sin^2(\varphi)\right) \qquad (8)$$

with P_{THz}^{LAQD} from Eq.s (2) – (6).

The previous considerations apply to a (hypothetical) large area quasi dipole (LAQD) embedded into an infinite bulk semiconductor. In a typical scenario, however, the absorption of the laser radiation will take place in the semiconductor close to its interface to air at z = 0. The radiation pattern of Hertzian dipoles placed in a semiconductor close to the surface (distance $z_0 << \lambda$) is expected to differ significantly from the one embedded within the infinite bulk. Therefore, in the following Section III, the angular power distribution for the case of a vertical and horizontal Hertzian dipole at the interface to air, $U_v^{LAQD,if}(\theta)$, and for the case of a horizontal dipole, $U_h^{LAQD,if}(\theta,\varphi)/d\Omega$, will be developed.

In order to fully take advantage of the large area emitter (LAE) concept, the dimensions of the illuminated area will typically be chosen comparable with the THz wavelength (in the semiconductor), λ_0/n_{sc}, or even larger. In this case, interference effects will influence the angular dependence of the radiation pattern. This situation is being treated in Sections

IV and V for the two field orientations. In order to establish the close connection of such LAEs to the antenna emitter arrays (AEA)s we will first subdivide the actual "continuous array" of elementary Hertzian dipoles into a discrete, but sufficiently dense array of Hertzian dipoles of correspondingly enhanced dipole charge, yielding an array factor for large area emitters, $AF_{LAE}(\rho_0,\theta,\varphi)$, depending on their characteristic dimension, ρ_0, similar to the one developed in Section IV of Part I of this paper. The actual angular dependence of the radiation intensity at vertical DC E-fields, $U_v^{LAE}(\theta,\varphi)$, and in-plane DC E-fields, $U_h^{LAE}(\theta,\varphi)$, will then, again, be given by the product of the angular dependence of the (modified) Hertzian dipole patterns and the array factors

$$U_h^{LAE}(\theta,\varphi) = U_h^{LAQD,if}(\theta,\varphi) \cdot AF^{LAE}(\theta,\varphi) \tag{9}$$

and

$$U_v^{LAE}(\theta,\varphi) = U_v^{LAQD,if}(\theta) \cdot AF^{LAE}(\theta,\varphi) \tag{10}$$

respectively.

ACKNOWLEDGEMENTS

This work was partially granted by CICYT NeoImag TEC2009-14525-C01 and CONSOLIDER-INGENIO 2010 CSD2008-00068. The work of Javier Montero-de-Paz was supported by the Spanish Education Minister under the program FPU (AP2009-4679). The work of Eduardo Ugarte-Muñoz was supported by the Spanish Economy Minister under the program FPI (BES2010-037676). Prof. G. Dohler work was granted by "Cátedras de Excelencia" from Banco Santander. Authors also would like to thanks Prof. David M. Pozar and Prof. David B. Rutledge for their constructive comments.

REFERENCES

[1] S. Preu, G.H. Döhler, S. Malzer, L.J. Wang, H. Lu, and A.C. Gossard, "Tunable, Continuous Wave Terahertz Photomixer Sources and Applications" (review article), *Journal of Applied Physics*, Vol. 109, 2011.

[2] M. Kominami, D. M. Pozar, D. H. Schaubert, "Dipole and Slot Elements and Arrays on Semi-Infinite Substrates", *IEEE Trans. on Antennas and Propagation*, Vol. AP-33, No. 6, pp. 600-607, June 1985.

[3] D. B. Rutledge, D. P. Neikirk, D. P. Kasilingam, "Integrated-Circuit Antennas", *Infrared and Millimeter Waves. Vol 10, Millimeter Components and Techniques Part II*, K. J. Button, Ed. New York: Academic, 1983.

[4] W. Lukosz, and R. E. Kunz, "Light emission by magnetic and electric dipoles close to a plane interface. Part I. Total Radiated Power. Part II. Radiation pattern of perpendicular oriented dipoles. Part III. Radiation pattern of dipoles with arbitrary orientation", *Journal of the Optical Society of America*, Vol. 67, No. 12, pp. 1607-1615, December 1977.

[5] D. F. Filipovic, S. S. Gearhart, G. M. Rebeiz, "Double-Slot Antennas on Extended Hemispherical and Elliptical Silicon Dielectric Lenses," *IEEE Transactions on Antennas and Propagation*, vol. 41, no. 10, October 1993.

[6] Airy, G. B., "On the Diffraction of an Object-glass with Circular Aperture", Transactions of the Cambridge Philosophical Society 5, 283 (1835).